
수중음향통신을 위한 광대역 FIR 빔형성기

최영철* · 임용곤*

A Broadband FIR Beamformer for Underwater Acoustic Communications

Youngchol Choi* · Yong-kon Lim*

요 약

수중음향통신을 위한 빔형성 기법은 대역폭이 반송주파수에 비해서 큰 광대역 신호 특성을 고려해야 한다. 수중음향통신에서는 협대역 신호 가정이 성립하지 않는다. 본 논문에서는 기저대역 배열신호 모델을 이용한 수중음향통신 광대역 FIR 빔형성기에 대해서 논한다. 반송주파수 25kHz, 심볼 속도 5kHz인 QPSK 방식의 수중음향통신에 있어서 광대역 FIR 빔형성기를 고려했다. 배열 센서는 8개의 등방형 센서로 구성된 선형등간격 구조이고, 센서간 간격은 반송주파수 파장의 절반이다. 컴퓨터 모의실험을 통하여 각 센서에 길이가 2인 FIR 필터를 채택하고 탭간 간격이 심볼 주기의 1/4일 때 광대역 FIR 빔형성기는 최적 신호 대 간섭잡음비에 근접하였으며, 기존의 통상적인 협대역 빔형성기보다 신호 대 간섭잡음비가 0.5dB 향상된 결과를 보였다. 광대역 FIR 빔형성기의 성능은 FIR 필터 길이가 특정 값 이상으로 커지면 더 나빠지고, 탭간 간격이 심볼 주기의 절반보다 작으면 탭간 간격은 성능에 영향을 주지 않았다. 탭간 간격이 심볼 주기와 같은 경우에, 훈련 신호열이 통상적인 경우보다 더 많이 필요하였다.

ABSTRACT

Beamforming for underwater acoustic communication (UAC) is affected by the broadband feature of UAC signal, which has relatively low carrier frequency as compared to the signal bandwidth. The narrow-band assumption does not hold good in UAC. In this paper, we discuss a broadband FIR beamformer for UAC using the baseband equivalent array signal model. We consider the broadband FIR beamformer for QPSK UAC with carrier frequency 25kHz and symbol rate 5kHz. Array geometry is a uniform linear array with 8 omni-directional elements and sensor spacing is the half of the carrier wavelength. The simulation results show that the broadband FIR beamformer achieves nearly optimum signal to interference and noise ratio (SINR) and outperforms the conventional narrowband beamformer by SINR 0.5dB when two-tap FIR filter is employed at each sensor and the inter-tap delay is a quarter of the symbol interval. The broadband FIR beamformer performance is more degraded as the FIR filter length is increased above a certain value. If the inter-tap delay is not greater than half of the symbol period, SINR performance does not depend on the inter-tap delay. More training period is required when the inter-tap delay is same as the symbol period.

키워드

수중음향통신, 배열 센서 신호처리, 광대역 빔형성기, 신호 대 간섭잡음비

I. INTRODUCTION

The electromagnetic wave is inappropriate for underwater

wireless communications because of the rapid attenuation in underwater environments such as the ocean. However the acoustic wave can propagate relatively long range compared

with the electromagnetic wave and it makes the acoustic wave be widely used for underwater wireless communications.

From a communicative point of view, underwater acoustic channel is different from the well-known radio frequency channel characteristics in air, which are resulted from the different medium (air and sea water) and the physical difference of the acoustic and electromagnetic wave[1, 2, 3]. It is the most distinctive characteristics of underwater acoustic channel that the slow propagation speed of the acoustic wave makes the complicated multi-path propagation phenomena to be up to several milisecond equivalent to tens of symbols in the horizontal high-rate UAC systems. The magnitude of some multi-path is close to that of the direct path, especially the ones reflected at the surface and bottom only one time. Doppler fluctuation is induced by the ocean current and random movement of the transceivers.

In the last two decades, there are many attempts to overcome the limits of UAC channel[2]. The compensation strategy for UAC channel distortion can be classified into temporal signal processing including equalizer and spatial signal processing including beamformer and diversity, or combination of them. The disadvantage of an adaptive equalizer is that the algorithm parameter should be re-fitted according to the change of the channel environments. The equalizer length should be very long to cover the extended multi-paths, so it is unsuitable for the real-time implementation. In addition, the throughput is reduced by the need for larger training symbols to guarantee the convergence of an adaptive algorithm. On the contrary, beamformer is robust on the change of channel environments and only dependent on the spatial distribution of multi-paths. Also, SNR is improved by the beamforming process when the noise is spatially uncorrelated.

In commercial air communication systems, radio frequency communication signal is narrow, i.e., bandwidth to carrier frequency ratio (BCR) is very small and it is suitable to assume narrow-band signal for beamforming. But beamforming for UAC is affected by the broadband feature of UAC signal, which has the relatively low carrier frequency compared with the signal bandwidth. Most of UAC system uses frequency band in 20kHz~100kHz and the typical

bandwidth is not greater than 10kHz in a high-rate long-range transmission because of the absorption loss of acoustic wave in sea-water which is proportional to the frequency in dB scale and it makes BCR be in the range of 0.1~0.5. Therefore, the narrow-band assumption does not hold good in UAC.

Broadband digital beamforming algorithm can be implemented in the frequency domain or time domain, which is called discrete fourier transform (DFT) beamformer and broadband FIR beamformer, respectively. It is well known that they are equivalent to each other[4]. Broadband FIR beamformer performance is influenced by the BCR[5]. Signal to interference and noise ratio (SINR) is degraded by the increase of BCR and SINR reduction is less than 1dB compared with zero BCR when the inter-tap delay is smaller than the suggested value and FIR filter length for each sensor is large enough. Unfortunately, the results of [5] are restricted to pass-band beamforming and discussed with the impractical conditions in communications such as signal to interference ratio (SIR) -40dB and signal to noise ratio (SNR) 0dB.

In this paper, we consider a broadband FIR beamformer for UAC based on the baseband equivalent array signal model and discuss the performance of a broadband FIR beamformer for UAC by computer simulations with practical conditions. In the section II, we derive the baseband equivalent vector signal model for the broadband FIR beamformer of phase-coherent UAC system. In the section III, computer simulation results are shown for QPSK UAC system with carrier frequency 25KHz and symbol rate 5KHz, and conclusions are followed.

II. SIGNAL MODEL

Consider a broadband FIR beamformer for UAC with the uniform linear array (ULA) sensor as fig. 1, where N is the length of the FIR filter, M is the number of the elements of the array and $w_{i,j}$ is the j th tap weight of the i th sensor. The quadrature demodulated output of each sensor is filtered by FIR filter and summed to perform broadband beamforming. The FIR filtering process compensates the broadness of UAC signal.

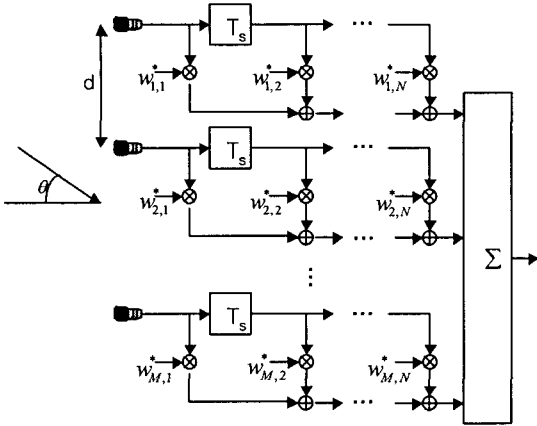


그림 1. 광대역 FIR 빔형성기 구조
Fig. 1. Broadband FIR beamformer structure

We list some notations to be used as follows.

Notation

- f_c : Carrier frequency
- $x_I(t)$: In-phase signal in baseband
- $x_Q(t)$: Quadrature-phase signal in baseband
- $x(t) = x_I(t) + jx_Q(t)$: Complex envelop
- N : FIR filter length
- T : Symbol interval
- T_s : Inter-tap delay
- M : Number of sensors
- d : Sensor spacing
- θ : Incidence angle
- c : Sound speed

The received passband signal at the first sensor $x_{P_1}(t)$ can be written as

$$\begin{aligned} x_{P_1}(t) &= \text{Re} \{ x(t) e^{j2\pi f_c t} \} \\ &= x_I(t) \cos(2\pi f_c t) - x_Q(t) \sin(2\pi f_c t) \end{aligned} \quad (1)$$

Then the received passband signal at the m th sensor

$x_{P_m}(t)$ with incidence angle θ is

$$x_{P_m}(t) = x_{P_1}(t - (m-1)\tau), \quad \tau(\theta) = \frac{d \sin \theta}{c} \quad (2)$$

The complex envelope at the m th sensor $x_m(t)$ can be obtained by frequency conversion and low-pass filtering as follows,

$$\begin{aligned} x_m(t) &= x_{m_I}(t) + jx_{m_Q}(t), \quad (3) \\ x_{m_I}(t) &= x_I(t - \tau_m) \cos(-2\pi f_c \tau_m) - \\ &\quad x_Q(t - \tau_m) \sin(-2\pi f_c \tau_m) \\ x_{m_Q}(t) &= x_I(t - \tau_m) \sin(-2\pi f_c \tau_m) + \\ &\quad x_Q(t - \tau_m) \cos(-2\pi f_c \tau_m) \end{aligned}$$

where $\tau_m = (m-1)\tau$. The above equations can be rewritten in the matrix form

$$\begin{pmatrix} x_{m_I}(t) \\ x_{m_Q}(t) \end{pmatrix} = \begin{pmatrix} \cos(-2\pi f_c \tau_m) & -\sin(-2\pi f_c \tau_m) \\ \sin(-2\pi f_c \tau_m) & \cos(-2\pi f_c \tau_m) \end{pmatrix} \times \begin{pmatrix} x_I(t - \tau_m) \\ x_Q(t - \tau_m) \end{pmatrix} \quad (4)$$

Note that the first term of the right-hand side in the above equation is a rotation matrix. Then the above matrix form can be rewritten in the complex domain as follows

$$x_m(t) = x(t - \tau_m) e^{-j2\pi f_c \tau_m}$$

It is clear from the above equation that the complex envelope of the m th sensor is the time delayed and rotated version of the complex envelope of the first sensor. Therefore the received complex envelope array signal with incidence angle θ can be written in vector form

$$\begin{aligned} \begin{pmatrix} x_1(t) \\ \vdots \\ x_m(t) \\ \vdots \\ x_M(t) \end{pmatrix} &= \begin{pmatrix} x(t) \\ \vdots \\ x(t-\tau_m)e^{-j2\pi f_c \tau_m} \\ \vdots \\ x(t-\tau_M)e^{-j2\pi f_c \tau_M} \end{pmatrix} \\ &= A(\theta) \begin{pmatrix} x(t) \\ \vdots \\ x(t-\tau_m) \\ \vdots \\ x(t-\tau_M) \end{pmatrix} \end{aligned} \tag{5}$$

where $A(\theta) = \text{diag}(1, \dots, e^{-j2\pi f_c \tau_M})$ and $\text{diag}(a_1, \dots, a_n)$ denotes $n \times n$ diagonal matrix. Note that $A(\theta)$ is the diagonal matrix correspond to the array response vector in the conventional narrowband beamformer. Finally, the $M \times N$ received data matrix Y with K multi-paths can be described as follows

$$Y = \sum_{k=1}^K A(\theta_k) X(t-t_k, \theta_k) \tag{6}$$

where

$$X(t-t_k, \theta_k) = \begin{pmatrix} \underline{x}^T(t-t_k) \\ \vdots \\ \underline{x}^T(t-t_k-\tau_{k,m}) \\ \vdots \\ \underline{x}^T(t-t_k-\tau_{k,M}) \end{pmatrix},$$

$$\underline{x}^T(t) = (x(t) \dots x(t-(N-1)T_s)),$$

t_k is the time delay of the k th path, θ_k is the incidence angle of the k th path and $(\cdot)^T$ denotes the matrix transpose, where $\tau_{k,m} = (m-1)\tau(\theta_k)$. Note that $X(t-t_k, \theta_k)$ consists of the row vector which denote the received complex envelope of each sensor. In the next section, we will determine the optimal inter-tap delay T_s and the FIR filter length N by computer simulations using the above baseband equivalent vector signal model.

III. SIMULATION RESULTS

In this simulation, we consider a vertical ULA with 8 omni-directional elements and QPSK UAC system with carrier frequency 25KHz and symbol rate 5KHz. Pulse shaping filter is the raised cosine filter with roll-off factor 0.25. Hence BCR is 0.25. The sensor spacing is the half of the carrier wavelength. For simplicity, we assume that there is no signal fading and synchronizations are perfect. We have considered two propagating paths: direct and surface reflected ones. The surface reflected path is regarded as the interference signal. SNR and SIR are fixed to 6dB and 0dB, respectively. The propagation paths could be restricted to direct and surface or bottom reflected ones in the horizontal acoustic channel of the ocean. For example, if the transducers are suspended from surface at 100m depth and transmission range is 1Km in the deep ocean with 1Km depth, the surface reflected path has relative amplitude to direct path 0.98 with time delay 13ms correspond to 65 symbols period. The bottom reflected path is negligible because of the absorption at the bottom.

We assume that the direct path is incident at broadside and the incidence angle of the surface reflected path is varying from -90° to 90° . RLS algorithm is used to adaptively update tap weights. We discuss the SINR performance of the broadband FIR beamformer by changing the inter-tap delay $T_s = T/L$, $L = 1, 2, 4$ and FIR filter length N .

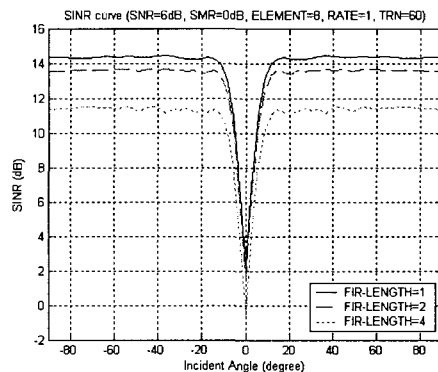


그림 2 탭간 간격이 심볼 주기와 같은 경우의 SINR 곡선
Fig. 2. SINR curves when the inter-tap delay is equal to the symbol period.

Fig. 2 is SINR curves for $N = 1, 2, 4$ when $L = 1$, i.e., the inter-tap delay is same as the symbol period. Fig. 2 shows that the broadband FIR beamformer is the best when $N = 1$ which is equivalent to the conventional narrow-band beamformer. SINR performance is more degraded by the increase of N . These results are different from those of [5] which showed that SINR was reduced about 10dB when $BCR=0.25$ and $N = 1$ and performance degradation was negligible when N was greater than a certain value which was function of BCR. The different assumption makes the difference. In [5], SIR and SNR are fixed at -40dB and 0dB , respectively, which are impractical in UAC channel.

Usually, RLS algorithm converges after iterations of two times of FIR filter length but the simulation results show that more training period is required when $L = 1$. At least 60 symbols are required as a training sequence when $L = 1$, but 20 symbols are enough to achieve the best performance when $L = 2, 4$.

Fig. 3 shows SINR curves for $N = 1, 2, 3, 4$ when $L = 2$, i.e., the inter-tap delay is the half of the symbol period. When $L = 2$, the SINR performance is similar to the case of $L = 1$ as seen from fig. 2 and fig. 3 except for the required length of the training sequence.

Somewhat different results are appeared when $L = 4$ as seen from fig. 4. SINR is decreased by increasing N when $L = 1, 2$ but SINR is maximum at $N = 2$ and decreased for N greater than 4. The maximum SINR is about 14.8dB and this value is nearly optimum because SNR should be improved 9dB with 8-elements sensor array in the additive white Gaussian noise channel.

From the above discussions, we can conclude that $L = 4$ and $N = 2$ is the best choice for the broadband FIR beamformer for UAC with carrier frequency 25KHz and bandwidth 5KHz and SINR is improved by 0.5dB as compared to the conventional narrowband beamformer. Also, SINR is reduced when the FIR filter length is larger than a certain value and SINR performance is not dependent on the inter-tap delay if it is remained small enough. Note that the similar results are observed although the BCR is increased.

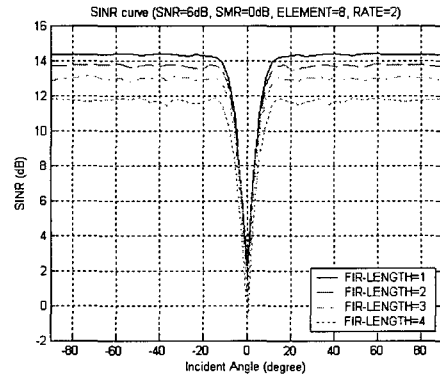


그림 3. $L=2$ 인 경우의 SINR 곡선
Fig. 3. SINR curves when $L=2$

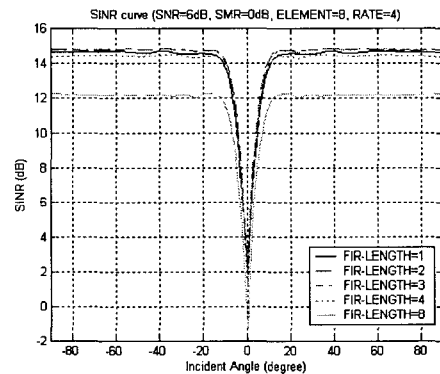


그림 4. $L=4$ 인 경우의 SINR 곡선
Fig. 4. SINR curves when $L=4$

IV. CONCLUSIONS

The baseband equivalent signal model is derived for a broadband FIR beamformer and it is shown that the broadband FIR beamformer achieves nearly optimum SINR and outperforms the conventional narrowband beamformer by 0.5dB of SINR in QPSK UAC system with carrier frequency 25KHz and symbol rate 5KHz when two-tap FIR filter is employed at each sensor and the inter-tap delay is a quarter of the symbol interval. SINR performance is more degraded as the FIR filter length is more and more larger than a certain value and the effect of inter-tap delay is negligible if it is kept short enough. When the inter-tap delay is same as the

symbol period, more training period is required to guarantee the convergence of the RLS algorithm.

ACKNOWLEDGMENT

This work is based on the projects "Development of UA-Net", supported by Ministry of Maritime Affairs & Fisheries (MOMAF) and "Development of Underwater 3D Fusion Image Reconstruction and Acoustic-Based Communication Technology", supported by Korea Research Council of Public Science and Technology (KORP).

REFERENCES

- [1] L. Brekhovskikh and Y. Lysanov, *Fundamentals of Ocean Acoustics*. New York: Springer Verlag, 2003.
- [2] D. Kilfoyle and A. Baggeroer. "The state of the art in underwater acoustic telemetry," *IEEE J. of Oceanic Eng.*, Vol. 25, pp. 4-27, Jan. 2000..
- [3] Y. Park and J. Yim, "A study on the protocol design and implementation for an underwater acoustic multi-channel digital communication," *Journal of KIMICS*, Vol. 4, No. 1, pp. 179-189, 2000.
- [4] H. Van Trees, *Optimum Array Processing*, New York: John Wiley & Sons, 2002.
- [5] F. Vook and R. Compton, "Bandwidth performance of linear adaptive arrays with tapped delay-line processing," *IEEE Trans. AES*, Vol. 28, No. 3, pp. 901-908, July 1992.

저자소개



최 영 철(Youngchol Choi)

1998년 KAIST 전기및전자공학과 (공학사)

2000년 KAIST 전기및전자공학과 (공학석사)

2006년 12월 현재 한국해양연구원 연구원

※관심분야: 수중음향통신 및 신호처리



임 용 곤(Yong-kon Lim)

1979년 충남대학교 전기공학 (공학사)

1984년 충남대학교 전기공학 (공학석사)

1994년 아주대학교 전자공학(공학박사)

2006년 12월 현재 한국해양연구원 책임연구원

※관심분야: 수중음향통신, 수중 로봇, 해양 물류, 유 비쿼터스, Ad-hoc 네트워크, 센서 네트워크